Mon. Not. R. Astron. Soc. **370,** 1556–1564 (2006) doi:10.1111/j.1365-2966.2006.10578.x

15-GHz variability of 9C sources

R. C. Bolton,[1⋆] C. J. Chandler,[2] G. Cotter,[3] T. J. Pearson,[4] G. G. Pooley,[1⋆] A. C. S. Readhead,[4] J. M. Riley[1⋆] and E. M. Waldram[1⋆]

[1]*Cavendish Astrophysics, Department of Physics, J. J. Thomson Avenue, Cambridge CB3 0HE*
[2]*National Radio Astronomy Observatory, PO Box 0, Socorro, NM 87801, USA*
[3]*Oxford Astrophysics, Denys Wilkinson Building, Keble Road, Oxford OX1 3RH*
[4]*California Institute of Technology, 1201 East California Blvd, Pasadena, CA 91125, USA*

Accepted 2006 May 17. Received 2006 April 20; in original form 2005 September 29

ABSTRACT

We present results from a 3-yr study of the 15-GHz variability of 51 9C sources. 48 of these sources make up a subsample of a larger one complete to 25 mJy in 9C, and as the sources are selected pseudo-randomly the results should be representative of the complete sample. 29 per cent of this subsample are found to be variable above the flux calibration uncertainties of ∼6 per cent. 50 per cent of the flat-spectrum objects are variable whilst none of the steep-spectrum objects or the objects with convex spectra peaking below 5 GHz are variable. Nine of the objects studied have convex spectra and peak frequencies above 5 GHz; eight of these were found to vary at 15 GHz, suggesting that the high-frequency peaking class in this sample is largely populated by objects with jets aligned close to the line of sight whose emission is dominated by beamed components.

Key words: surveys – galaxies: active – radio continuum: general.

1 INTRODUCTION

The 9th Cambridge survey (9C; Waldram et al. 2003) has been carried out at 15 GHz with the Cambridge Ryle Telescope (RT; Jones 1991). The main scientific motivation for 9C was the need to identify foreground sources that could contaminate cosmic microwave background (CMB) maps from the Very Small Array (VSA; e.g. Taylor et al. 2003), a CMB telescope operating at 34 GHz. 9C was carried out by performing blind raster scans of the sky at 15 GHz and then following up possible detections from the raster maps with pointed observations (again at 15 GHz) to confirm the detection and measure the source flux density or to rule it out.

Extensive radio and optical follow-up of 176 sources from 9C has been presented in Bolton et al. (2004) (Paper 1 hereafter), and this provides a simultaneous continuum radio spectrum spanning 1.4–43 GHz for each object, as well as an optical identification for ∼90 per cent of them. 19 per cent of the follow-up sources in a sample complete to 25 mJy in 9C had spectra with peak frequencies between 0.5 and 10 GHz, double the fraction found in lower frequency (e.g. 5 GHz) surveys (O'Dea 1998).

Synchrotron self-absorption models suggest that compact young radio sources (younger than a thousand years or so) should have synchrotron spectra peaking at a few gigahertz or above (O'Dea 1998; Snellen et al. 2000). If a significant fraction of the gigahertz-peaked spectrum (GPS) and high-frequency peaked (HFP) objects found in 9C are genuinely young objects they will provide insights into the mechanisms that trigger radio sources and their early evolution.

From the initial follow-up data, it is unclear what proportion of the sample of HFP objects is made up of beamed objects that are not necessarily either compact or young. Since beamed objects are likely to have variable flux density at high radio frequency, whilst genuinely young, unbeamed objects should be stable (or possibly slowly increasing) in flux density, monitoring of the flux density of the HFP objects should help to identify beamed objects.

We also consider whether variability can affect the VSA observations. For example, in the first VSA observations with the compact array, for the VSA confusion noise to be significantly lower than the flux sensitivity (≃30 mJy) Taylor et al. (2003) state that they must subtract all sources brighter than 80 mJy at 34 GHz. In order to achieve this, during the VSA observations, all sources brighter than ∼20 mJy in 9C were observed by the VSA source subtractor telescopes that operate at the same frequency as the VSA. If sources have varied in flux density so that they are fainter during the VSA observations than they were during the initial raster scans or pointed observations of 9C, then this will not compromise the CMB data; however, any sources which either were too faint to be detected at the time of the 9C raster scans, or have flux densities in 9C below the cut-off for study with the source subtractor telescopes, but whose flux densities have since increased, will add uncorrected noise to the CMB data. It is therefore desirable to study the variability of 9C sources at centimetre wavelengths to establish whether or

⋆E-mail: r.c.bolton.97@cantab.net (RCB); guy@mrao.cam.ac.uk (GGP); julia@mrao.cam.ac.uk (JMR); emw1@mrao.cam.ac.uk (EMW)

not variability is likely to lead to serious incompleteness in the VSA source subtractor sample.

Subarcsecond resolution radio mapping of the compact 9C sources from one region of the complete 25-mJy sample of Paper 1 is presented in Bolton et al. (2006) (Paper 2 hereafter). This high-resolution mapping showed that almost all (16/17) sources with fitted peak frequencies above 0.5 GHz (in the observed frame) and 60 per cent of the flat-spectrum objects were unresolved at 3-mas resolution.

In this paper, we present a study of the 15-GHz flux density variability of a sample of 51 radio sources from the 9C survey, taken from Paper 1. Of the 51 sources studied in this paper, 48 were selected from the complete 25-mJy sample (sample A) from Paper 1; no consideration was given to spectral shape but sources close to each other on the sky were chosen to increase the efficiency of the observations. Because sources were selected in a pseudo-random manner, the sample studied here should be representative of the whole 25-mJy sample.

A further three HFP sources from sample C of Paper 1 were monitored because they happened to fit well into the observing programme. The sources in sample C had originally been selected from 9C on the basis that they were likely to be GPS or HFP sources, but they either were outside the area covered by the complete sample or had flux densities lower than the complete sample selection limit.

The layout of this paper is as follows. The observations and data reduction are described in Section 2; the method and results of measuring the variability of each source are shown in Section 3. In Section 4, the variability results are discussed with reference to the radio spectral type of the sources and the variability time-scales are considered. The implications of the results for the VSA observations and sample completeness are discussed in Section 5. A summary and discussion of the results from this work and from Papers 1 and 2 is given in Section 6.

2 OBSERVATIONS AND DATA REDUCTION

The study of the variability of 9C sources was carried out with the RT, with 51 sources observed frequently, but at irregular intervals, between 2003 June and 2005 April. The data obtained, in combination with the original 9C survey data (1999 November–2001 June) and the multifrequency follow-up of Paper 1 (2001 January–2002 May), give 15-GHz flux density measurements separated by time-scales of a few days to between 1.5 and 5 yr.

Observations were made in batches; the targets in each observing run consisted of six or seven sources close together on the sky, and an appropriate phase calibrator. In each observing run, approximately 15 min was spent on each source and the resulting rms thermal noise is between 1 and 2 mJy.

The RT has linearly polarized feeds, and so measures the combined Stokes' parameters I+Q. Flux calibration of the RT is carried out using 3C286 ($S_{15} = 3.5$ Jy) and 3C48 ($S_{15} = 1.7$ Jy). In Paper 1, we assumed that the day-to-day calibration of the RT flux-density scale was consistent with 3 per cent rms (Pooley & Fender 1997). However, as part of this variability study, we checked the accuracy of this day-to-day calibration by examining the archive data for the phase calibrator source 2005 + 403, which was observed on an almost daily basis during the epoch of the variability observations. We looked at the fractional rms deviation in the RT estimates of the flux density of 2005 + 403 over short periods of time (<25 d) since the source is itself variable. These data indicate that the fractional rms deviations over the epoch of this study are rather larger than 3 per cent, being typically between 4.5 and 6 per cent. Whilst this may in part be due to real variations in the source flux density on time-scales of a few days there are some indications that the telescope tracking may be slightly less accurate than it was. In this study, we take a conservative estimate of the accuracy of the day-to-day calibration of 6 per cent rms.

The data initially showed correlated variations in the fluxes from sources from the same observing runs. In particular, there were flux density drops at times coincident with wet weather. However, poor weather also resulted in increased noise on the phase calibrators so this was used to flag bad observations. All data taken during runs where the rms variation per 32-s sample on the phase calibrator was greater than 2.5 times the thermal noise limit of 6 mJy were discarded as this was found to be a reasonable choice for separating 'good' and 'bad' data.

3 TESTING FOR VARIABILITY

To test for variability a χ^2 test was carried out on the 'good' data for each source assuming the null hypothesis (H_0) that the ith source flux density measurement is taken from a distribution of constant mean $\overline{s}$ and standard deviation δ_i (where $\overline{s}$ is the weighted mean of all 'good' data points and δ_i is the uncertainty on the ith measurement, with the error resulting from the six per cent flux calibration uncertainty added in quadrature to the rms noise). The χ^2 test allows us to quantify the probability, P_0, of obtaining the data if H_0 is true. If P_0 is greater than 1 per cent then the null hypothesis is not rejected and the objects are classed as not variable (NV). Objects with P_0 less than 1 per cent are classed as variable (V).

The value of χ^2 is given by

$$\chi^2 = \sum_{i=1}^{n} \frac{(s_i - \overline{s})^2}{\delta_i^2}, \tag{1}$$

where s_i is the ith measured flux density.

The fractional variation, $\Delta S/S \equiv \sqrt{\langle (s_i - \overline{s})^2 \rangle}/\overline{s}$, was not used to classify the objects, but the calculated values are shown in Table 1, along with a summary of the data for each source.

For 34 of the 51 sources studied the χ^2 test gives a null result at the 1 per cent level: there is no strong evidence of variability above the uncertainties. Examples of these 'non-variable' sources are shown in Fig. 1. The fractional variation of objects in the 'non-variable' class ranges from 2.9 up to 14.7 per cent and the median value is 6.1 per cent. 17 of the 51 sources are classed as variable, with convincing evidence for flux density variations. These have fractional variation between 8.4 and 70 per cent, and a median of 14 per cent. Examples of variable objects are shown in Fig. 2.

Four of the 34 'non-variable' sources have borderline classifications with P_0 between 0.01 and 0.1 (all of the other 'non-variable' sources have $P_0 > 0.1$). The sources are J0013+2834 (which has a fractional variability of 9.9 per cent); J0022+3250 (fractional variability 14.7 per cent); J0927+2954 (fractional variability 7.9 per cent) and J0942+3309 (fractional variability 7.9 per cent). The data for these four objects are shown in Fig. 3.

4 ANALYSIS OF RESULTS

4.1 Radio spectral type and variability

Sources have been classified by spectral shape by fitting a quadratic function to the simultaneous observations of Paper 1. Four classes

Table 1. χ^2 test results. The columns are: source name; observation period; the number of observations used; the value of the weighted mean (in mJy); the fractional variation (per cent); the χ^2 value; the variability class; spectral type and fitted peak frequency (in GHz: see Paper 2). The three sources marked with a* are from sample C.

Source name	Observation period	n	$\overline{S}$ (mJy)	$\Delta S/S$ %	χ^2	Variability class	Spectral type	Peak (GHz)
J0010+2619	2001 November 23–2005 March 03	25	70.1	2.9	5.7	NV	Steep	–
J0010+2650	2001 November 23–2005 March 03	26	35.4	7.2	27.4	NV	Flat	–
J0010+2717	2001 November 23–2005 March 03	26	27.3	9.0	33.6	NV	Flat	–
J0010+2838	2001 November 23–2005 March 03	25	39.9	20.3	201.4	V	Flat	–
J0010+2854	2001 November 23–2005 March 03	25	88.2	12.2	102.1	V	Flat	–
J0011+2928	2001 November 23–2005 March 03	25	49.8	4.7	12.7	NV	Steep	–
J0012+3053	2001 November 23–2005 March 03	20	17.4	16.8	65.9	V	Flat	–
J0012+3353	2000 February 21–2005 March 03	22	136.1	21.2	208.7	V	HFP	36.9
J0013+2646	2000 February 21–2005 March 03	22	28.6	5.2	9.4	NV	Steep	–
J0013+2834	2001 November 23–2005 March 03	19	27.3	9.9	30.5	NV	Flat	–
J0014+2815	2001 November 23–2005 March 03	19	42.1	10.5	64.9	V	Flat	–
J0015+3052	2001 November 23–2005 March 05	19	38.9	4.2	8.3	NV	Steep	–
J0015+3216	1999 October 18–2005 March 23	127	461.9	6.0	143.1	NV	Steep	–
J0019+2956	2003 July 17–2005 March 05	18	43.2	5.6	13.0	NV	GPS	1.2
J0019+3320	2003 July 17–2005 March 05	19	31.5	5.9	12.9	NV	GPS	1.2
J0020+3152	2001 November 27–2005 March 05	16	24.8	7.4	14.2	NV	GPS	4.9
J0021+3226	2001 November 27–2005 March 05	17	26.2	6.7	14.1	NV	Steep	–
J0022+3250	2001 November 27–2005 March 05	20	13.3	14.7	36.4	NV	Flat	–
J0023+2734	2001 November 27–2005 March 06	12	73.2	6.3	10.9	NV	Steep	–
J0023+3114	2001 November 27–2005 March 06	11	33.2	3.5	2.6	NV	Steep	–
J0024+2911	2000 February 22–2005 March 06	47	40.7	28.0	880.2	V	HFP	13.1
J0027+2830	2001 November 27–2005 March 06	13	24.4	6.4	8.5	NV	GPS	1.1
J0028+2914	2001 November 27–2005 March 06	14	76.6	4.9	8.5	NV	Steep	–
J0028+2954	2001 November 27–2005 March 06	13	26.8	9.4	16.6	NV	GPS	4.4
J0927+2954	1999 November 27–2005 March 31	47	28.9	7.9	60.5	NV	Flat	–
J0927+3034	2001 July 02–2005 March 31	37	42.4	5.3	22.4	NV	Flat	–
J0928+2904	1999 November 27–2005 March 31	49	25.7	7.1	45.9	NV	Steep	–
J0932+2837	2000 August 19–2005 March 31	59	57.9	4.2	27.6	NV	GPS	2.1
J0933+2845	1999 November 27–2005 March 31	45	28.5	7.0	38.8	NV	GPS	1.6
J0933+3254	2000 January 06–2005 March 31	49	21.3	13.0	107.4	V	Flat	–
J0934+3050	1999 November 27–2005 March 31	48	43.2	4.8	24.7	NV	Steep	–
J0935+2917	1999 November 27–2005 March 31	60	44.7	8.7	104.0	V	HFP	5.3
J0936+3207	1999 November 27–2005 March 31	40	37.8	10.1	84.8	V	HFP	16.8
J0937+3206	2000 January 06–2005 March 31	36	55.3	9.1	74.2	V	Flat	–
J0939+2908	2002 February 02–2005 March 31	57	63.2	33.8	877.0	V	Flat	–
J0940+3015	2003 August 10–2005 March 31	47	62.0	5.3	33.8	NV	Flat	–
J0942+3309	2002 February 09–2005 March 31	37	43.0	7.9	53.6	NV	Flat	–
J0945+3003*	2000 January 07–2005 March 31	45	12.6	15.5	85.2	V	HFP	16.0
J1459+4442*	2001 January 17–2005 April 21	27	166.0	14.4	101.2	V	HFP	8.4
J1501+4537*	2001 January 17–2005 April 21	25	6.5	70.6	206.2	V	HFP	11.3
J1502+3753	2003 June 04–2005 April 21	23	39.3	4.2	9.3	NV	Steep	–
J1502+3947	2003 June 04–2005 April 21	23	35.5	3.4	5.7	NV	Steep	–
J1506+3730	2002 January 11–2005 April 21	36	535.5	8.4	77.1	V	Flat	–
J1516+3650	2003 June 04–2005 April 21	23	96.7	6.5	23.9	NV	Flat	–
J1517+3936	2003 April 25–2005 April 21	24	31.4	10.7	52.3	V	Flat	–
J1519+3913	2002 January 12–2005 April 19	14	41.1	5.2	8.6	NV	Steep	–
J1520+3843	2002 January 12–2005 April 19	13	42.0	6.8	15.1	NV	Steep	–
J1526+3712	2002 January 12–2005 April 19	13	56.4	6.8	13.8	NV	HFP	6.8
J1528+3738	2002 January 12–2005 April 19	13	86.2	6.2	14.8	NV	Steep	–
J1528+3816	2002 January 12–2005 April 19	14	93.9	14.0	82.5	V	HFP	60.7
J1530+3758	2002 January 10–2005 April 19	13	59.6	6.2	11.4	NV	GPS	3.4

are defined in Paper 2, these are: GPS objects with convex spectra peaking between 0.5 and 5 GHz; HFP objects with convex spectra peaking above 5 GHz; flat-spectrum objects with fitted spectral index at 10 GHz, $\alpha_{10} < 0.5$ (we take $S \propto \nu^{-\alpha}$), and steep-spectrum objects with $\alpha_{10} \geqslant 0.5$. Full details of the classification scheme are given in Paper 2. The assigned spectral type for each source, and, for the GPS and HFP sources, the fitted peak frequency, are shown in Table 1.

Table 2 shows the numbers of variable and non-variable sources in each spectral class. No steep-spectrum or GPS sources are variable whilst 50 per cent of the flat-spectrum sources and eight out of the nine HFP objects have varied over the study period.

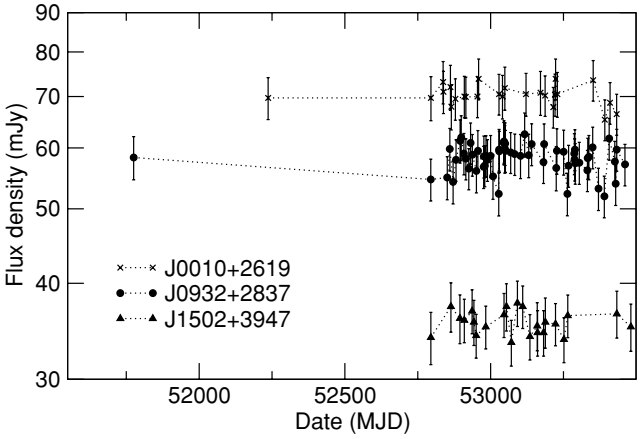

Figure 1. Examples of the variability study data for three stable sources. Data were taken between 2000 February 22 and 2005 March 06.

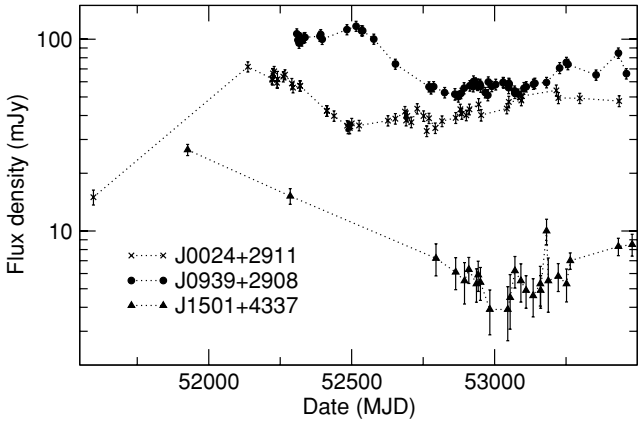

Figure 2. Examples of the variability study data for three highly variable sources.

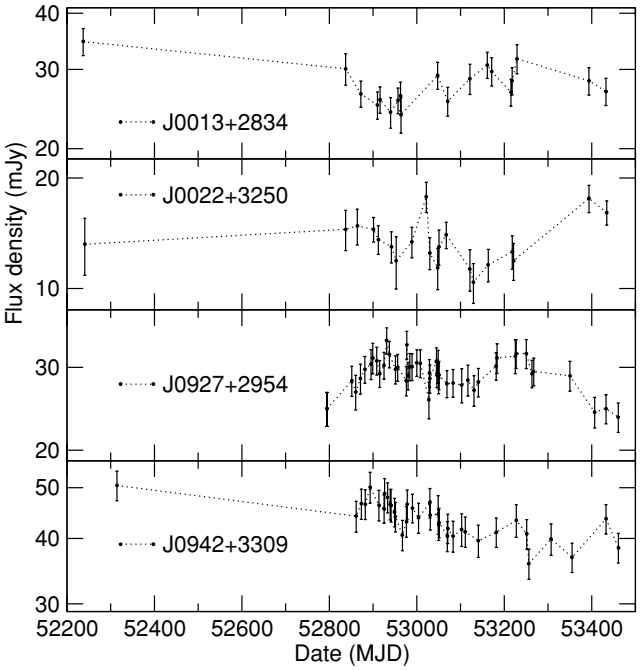

Figure 3. Examples of the variability study data for the four sources that have $0.1 > P_0 > 0.01$.

Table 2. Numbers of variable and non-variable sources in each spectral class; the three objects from sample C, all of which are variable and fall into the HFP class, have been included.

	HFP	Flat	GPS	Steep
Variable	8	9	0	0
Not variable	1	9	8	16

Peng at al. (2000) studied a complete, flux-limited sample of flat-spectrum sources (with flux density at 5 GHz greater than 1 Jy and $\alpha \leqslant 0.5$ between 2.7 and 5 GHz) and found that nine (69 per cent) of the 13 sources had $\Delta S/S > 7$ per cent over a 5-yr period. The 32 flat-spectrum GPS and HFP sources from the flux-limited sample presented here would probably all fall into Peng's 'flat-spectrum' class. Of these, 23 (72 per cent) have $\Delta S/S > 7$ per cent over $\sim$3 yr, in good agreement with the findings of Peng et al. in spite of the much lower flux limit. This comparison should be treated with some caution because the flux calibration uncertainty of the RT means that variability at the 7 per cent level is not necessarily significant.

4.2 Variability time-scales

The sources were observed at irregular intervals over the 2-yr period from 2003 June to 2005 April. There were also data available from the original 9C survey and the multifrequency follow-up. The χ^2 analysis in Section 3 allowed us to look at flux variations on time-scales greater than a few weeks over a period of between 1.5 and 5 yr.

The data are summarized in Fig. 4 in which the fractional variation for each source is plotted against the time interval spanned by the observations of that source. This shows that the proportion of sources which are significantly variable increases as the time-span increases and that this increase can be attributed entirely to variability of the flat-spectrum and HFP sources. Variability appears to occur at a higher level and to be much more common in the HFP sources than in the flat-spectrum ones (see also Table 2); however, given the dependence on time-span, the results for the two groups are not directly comparable as seven of the nine HFP sources have been observed over time-scales of more than 4 yr compared with only three of the 18 flat-spectrum sources.

To investigate the variability time-scales further, we have performed a structure function analysis (e.g. Simonetti, Cordes & Heeschen 1985) on the data for the individual variable sources. Following the procedure adopted by Hughes, Aller & Aller (1992), we plotted $\log D$ against $\log \tau$, where D is the first-order structure function and τ is the time lag, for each source. Although the data are sampled too sparsely and irregularly to enable us to comment in detail on the variability of each source, the analysis does provide some information on the variability time-scales up to about 2 yr. (Although values of D were obtained for longer time lags these depended largely on single flux density values obtained in the original survey or the follow-up and were therefore unreliable statistically). In the majority of cases, the plots of $\log D$ against $\log \tau$ have a plateau at short time lags consistent with the measurement noise and then show a steady increase in $\log D$ after a time lag of between 50 d and 1 yr. In all but two cases $\log D$ is still increasing after $\sim$2 yr indicating the variability time-scales are therefore longer than 2 yr. The plots for the sources 0024 + 2911 and 0939 + 2908 (the

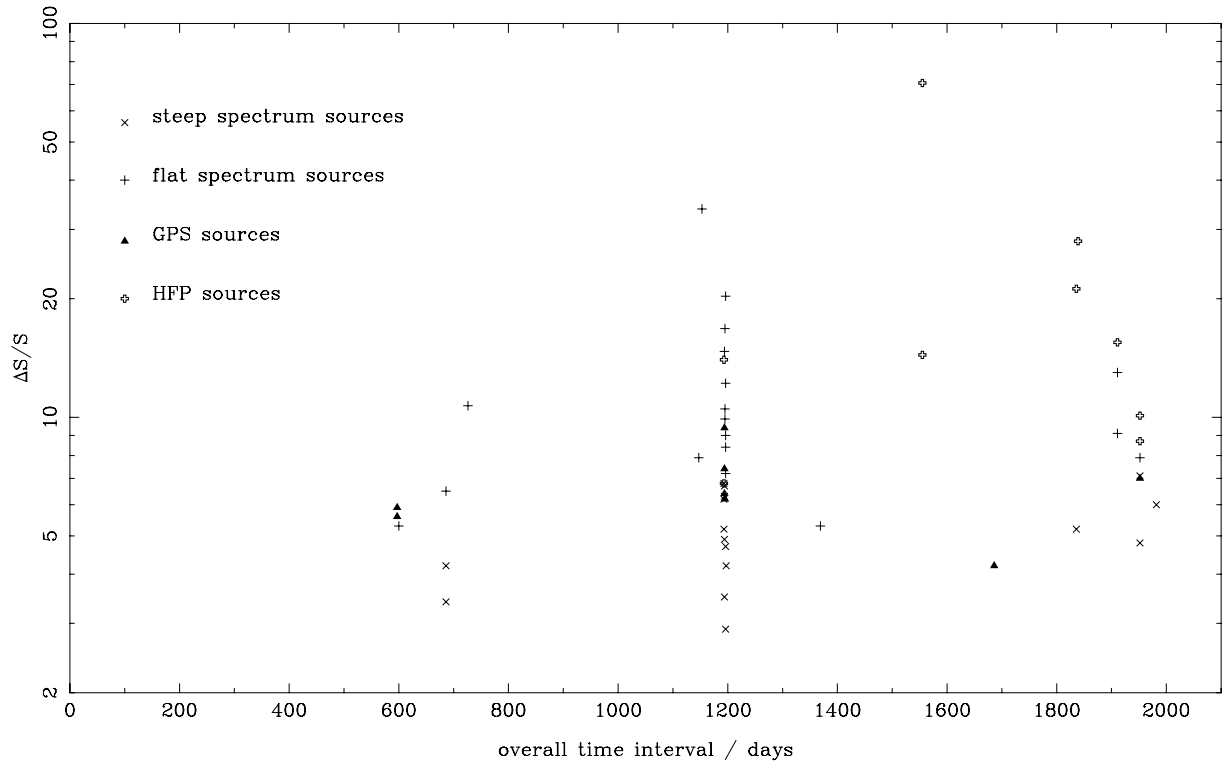

Figure 4. The fractional variation of each source plotted against the time interval spanned by the observations of that source. The symbols indicating the different spectral classes are, steep spectrum (×), flat spectrum (+), GPS (filled triangles) and HFP (open crosses).

two sources with the most extreme values of χ^2 in Table 1) show plateaus in log D after a time lag of ∼1.5 yr indicating slightly shorter variability time-scales in these two cases. There is no significant evidence for flux variations in any of the sources at a level greater than ∼6 per cent on time-scales less than ∼50 d.

5 IMPLICATIONS FOR SAMPLE COMPLETENESS

The variability data show that of the 48 sources selected from the 25-mJy flux-limited sample A, seven have flux densities that, for a significant fraction of the time, are less than 25 mJy (see the data for J1501 + 4337 in Fig. 2 for example). This suggests that there are likely to be a number of variable sources fainter than 25 mJy when the 9C observations were made which now have 15-GHz flux densities greater than 25 mJy. This will presumably not affect the statistics of the sample – the sample complete to 25 mJy in 9C should have the same properties as another 25-mJy sample selected from a blind survey at 15 GHz conducted at any other time. However, the high levels of variability displayed by some HFP objects confirm that care must be taken when using high-frequency surveys to identify possible contaminating foreground sources for CMB experiments at higher frequencies and later times.

Assuming that the number of sources increasing in flux density, but missing from 9C, is the same as the number decreasing in flux density and present in 9C, there are likely to be about 10 sources in the VSA fields which are now brighter than 25 mJy at 15 GHz, but are missing from the 9C catalogue.

The 15-GHz variability of some sources is as high as $\Delta S/S = 0.71$. It is therefore possible that a source could be missing from 9C because its flux density was just less than 25 mJy whilst the 9C observations were being made, but has almost doubled at 15 GHz to 43 mJy by the time of the VSA observations; with a spectral index of −0.75 between 15 and 34 GHz (the lowest spectral index seen in the objects studied here), it would have a flux density of 79 mJy at 34 GHz. This is very close to the 80-mJy flux limit for VSA source subtraction discussed in the introduction. However, only the most extreme spectral index and the highest fractional variability combined in one source would allow a source fainter than 25 mJy in 9C to be as bright as 80 mJy at 34 GHz a year or two later. Thus although the completeness of 9C is affected by variability, it is unlikely that point sources brighter than 80 mJy are contaminating the VSA data.

6 DISCUSSION

As mentioned in Section 1, the 'youth scenario' predicts that young, compact radio sources should be optically thick at low frequency; they should therefore have radio spectra peaking at gigahertz or few-gigahertz frequencies, with younger sources peaking at higher frequency than older, less-compact objects. For samples of GPS and compact steep-spectrum (CSS) sources, Snellen et al. (2000) find correlations between the peak frequency, peak flux and angular size which provide strong evidence for this picture. Additionally, there are examples of GPS objects with ages inferred from measured expansion speeds. These measurements indicate that they are genuinely young objects and lend considerable support to the youth scenario. For example, 0710 + 439 ($z = 0.518$) is a ∼1000-yr-old source with an observed spectrum peaking at ∼2 GHz and a physical size of ∼100 pc, and 2352 + 495 ($z = 0.238$) has an observed spectral peak at ∼1 GHz, a size of 100 pc and an inferred age of ∼2000 yr (Owsianik, Conway & Polatidis 1999, and references therein).

However, despite the evidence from the continuity in properties between GPS and CSS sources and between CSS sources and large-scale radio galaxies that these objects form an evolutionary sequence, there is as yet little convincing evidence that the HFP objects represent the earliest stage in this evolution. In particular, concerns have been raised about the contamination of GPS and HFP samples by beamed objects. Tinti and coworkers (Tinti et al. 2003, 2005) find that their sample of HFP objects (with peak frequencies above a few GHz) is largely contaminated by blazar objects, and, especially, that the majority of HFP sources associated with quasars are highly variable, probably beamed objects that happen to have emission dominated by a flaring, strongly self-absorbed component. They report a positive correlation between the peak frequency and the level of variability, in agreement with the results reported here. Torniainen et al. (2005) have also studied the variability on time-scales of about 20 yr of GPS and HFP sources associated with quasars. They find that all but five of the 35 inverted-spectrum sources they observed are strongly variable. The radio spectra of these sources change with time: in some the spectra remain convex whereas in others the spectra may at times be flat with an inverted spectrum only during flares. Torniainen et al. conclude that genuine, unbeamed GPS and HFP quasars are extremely rare and that, in order to find them, long-term flux-density monitoring is essential.

We now review the findings of all the 9C follow-up work and consider the results with reference to the nature of the 9C GPS and HFP objects in particular. The NASA/IPAC Extragalactic Database (NED) archives have been searched for all objects in Paper 1[1] and these data have been used to help improve our understanding of each source.

6.1 Variability in flat-spectrum, HFP and GPS objects

18 of the 51 objects studied here have flat radio spectra, and one half of these are variable. It is generally accepted that flat-spectrum objects owe their spectral shapes to relativistic beaming of different components in a jet closely aligned with the line of sight (LOS), and so variability in flat-spectrum objects is common.

The most striking result of this variability study is the difference in the levels of variability displayed by objects with observed spectral peaks above and below 5 GHz. Excluding the flat-spectrum objects, there are 24 GPS and steep-spectrum objects that peak below 5 GHz, if they peak at all, none of which are variable. However, eight of the nine objects that peak above 5 GHz are variable. The one source peaking above 5 GHz and not found to be variable in this study is J1526 + 3712; however, this shows evidence for long-term variability (especially at 5 GHz) in the NED archive data, shown in Fig. 5.

Tornikoski et al. (2001), in their long-term study of variability in GPS and HFP objects, find that objects exhibit more pronounced and higher frequency spectral peaks when they are in a flaring state than when they are in a quiescent phase. It is therefore possible that an object in a quiescent, non-variable phase will display a gigahertz-peaked or perhaps a flat spectrum and when it enters an active stage its spectrum peaks at high frequency. Although variability provides evidence for beaming the converse is not true – the absence of variability in an object does not imply that no beaming is occurring. Thus, some of the GPS sources in the sample studied here, which are currently showing no evidence for variability, may become HFP objects during times of activity.

[1] Plots of the spectra recovered from NED are available from the ftp site linked from http://www.mrao.cam.ac.uk/surveys/9C/

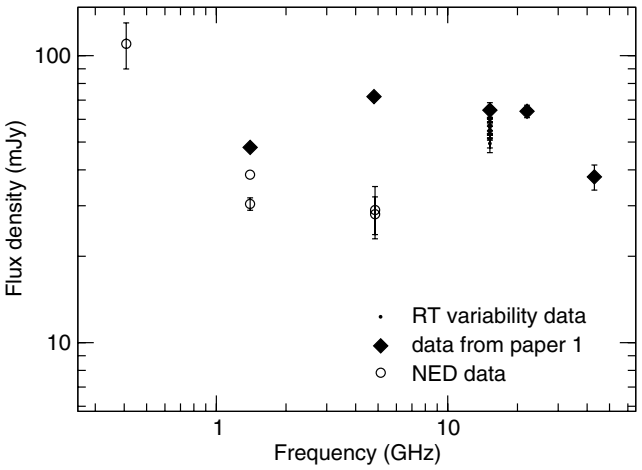

Figure 5. Data from the NED archive, Paper 1 and this paper for the source J1526 + 3712.

Table 3. Numbers of sources in each spectral class for samples A and B from Paper 1. The numbers in brackets are of sources resolved with the VLA and greater than 2 arcsec in angular extent.

	HFP	GPS	Flat	Steep	Total
Sample A	15 (1)	16 (0)	40 (7)	53 (31)	124
Sample B	13 (0)	11 (5)	23 (7)	23 (10)	70

6.2 The nature of the GPS and HFP objects

In this section, we examine the nature of the GPS and HFP objects. We use the data from the complete 9C samples presented in Paper 1, the angular size distribution of the sources in the 9C subsample discussed in Paper 2, and the variability data presented here along with the data from NED which provides information on variability over longer time-scales. We omit from the discussion any sources from the incomplete sample C.

The results of classifying all the sources by their spectral shape are shown in Table 3 for the two flux-limited samples from Paper 1 (sample A, complete to 25 mJy in 9C containing 124 objects and sample B, complete to 60 mJy and containing 70 objects). The angular sizes, or limits on the angular sizes, on arcsecond scales of all the sources in both samples have been measured with the Very Large Array (VLA) (see Paper 1); the numbers of sources with angular sizes larger than 2 arcsec in each spectral class are given in brackets in Table 3.

If we ignore the flat-spectrum objects, which we assume are beamed, it can be seen from Table 3 that there are roughly equal numbers of HFP and GPS sources in both samples, and that together they make up 37 per cent of sample A and 50 per cent of sample B. Snellen et al. (2000) suggest that the GPS phase in the life of a radio source lasts until it reaches a size of 1 kpc or so. In their model for this phase, the linear size L of a source grows in time t as $L \propto t^{1/2}$ and the peak frequency scales with time as $\nu_{\rm peak} \propto t^{-0.28}$. With these assumptions, the measured sizes and ages of the GPS sources 0710 + 439 and 2352 + 495 (Owsianik et al. 1999) mentioned earlier indicate that sources should be $\sim 10^4$–10^5 yr old when they reach 1 kpc in size; this is about one-thousandth of

the lifetime of a powerful radio source which is believed to be typically $\sim 10^7$–10^8 yr. Also, if HFP sources expand to become GPS sources, the HFP phase must last for $\ll 10^4$ yr. According to this analysis, the proportion of HFP and GPS sources in samples A and B seems large given their lifetimes relative to those of extended sources; additionally, from their lifetimes relative to each other, we would not expect to get equal numbers of HFP and GPS sources. These results therefore suggest that a number of the HFP and GPS objects in the samples are not part of an evolutionary sequence from HFP to GPS to CSS and eventually extended steep-spectrum objects. (More precise predictions of the relative numbers of sources in each phase for a flux-limited sample at a given frequency requires detailed modelling of the evolution of an individual source, the frequency at which it becomes optically thick and the cosmological evolution of the radio luminosity function).

Further support for this conclusion comes from the angular size distribution of the subsample of 61 sources studied in Paper 2 with subarcsecond resolution using the Multi-Element Radio-Linked Interferometer Network (MERLIN) and the Very Long Baseline Array (VLBA). This subsample is itself complete to 25 mJy in 9C and consists of all the sources in sample A from the 15^h 9C field; there are seven GPS sources and nine HFP sources in this subsample. Using lifetime arguments, many of the GPS sources would be expected to be of the order of 1 kpc in size – or at least $100 \sin\theta$ mas in projected angular extent (where θ is the angle between the jet and the LOS). The majority of such objects would be resolved with the VLBA. However, all the GPS sources in the sample in Paper 2 were unresolved even at 3-mas resolution (whilst all the steep-spectrum objects and one-third of the flat-spectrum objects were resolved with either the VLA, MERLIN or the VLBA). In order for these objects to remain unresolved with the VLBA, they must have projected linear sizes of less than 50 pc ($\sim$160 light-years) – half the projected sizes of 0710 + 439 and 2352 + 495. This requires that either they are younger than $\sim$500–1000 yr (by comparison with 0710 + 439 and 2352 + 495) or they are aligned closely with the LOS. It is statistically highly improbable that all the GPS objects in the sample in Paper 2 are aligned close to the LOS – unless, of course, they are beamed, which would simultaneously increase the chances of seeing such objects and remove the need to interpret their spectral shapes as signatures of youth. In the youth scenario, the sizes of the HFP sources are expected to be considerably smaller than those of the GPS sources. For example, extrapolating the data given by Snellen et al. (2000) sources with spectral turnovers at >5 GHz are expected to be typically less than $\sim$10 mas in extent. Nevertheless, if these sources did represent exclusively a population of very young sources, it is again surprising that the nine HFP sources in the sample in Paper 2 are also all unresolved at 3-mas resolution.

There is additional evidence pointing to the fact that most of the GPS and HFP sources are not young self-absorbed objects. We look first at radio variability. In addition to the 15-GHz variability observations presented here, variability at 1.4 GHz, over a time-scale of about 8 yr, has been investigated comparing the data from the NRAO (National Radio Astronomy Observatory) VLA Sky Survey (NVSS; Condon et al. 1998) with those given in Paper 1. Variability at 4.8 GHz, over a time-scale of about 15 yr, has also been examined using data from the GB6 catalogue of radio sources (Gregory et al. 1996). The results are presented in Table 4 which summarizes the properties of all the GPS and HFP sources in samples A and B. At both 1.4 and 4.8 GHz, any source for which the difference between the flux densities at the two epochs is more than three times their combined errors (σ_c) have been classed as variable (V); if the difference is between $2\sigma_c$ and $3\sigma_c$, the source is classed as possibly variable (PV) and if it is less than $2\sigma_c$ it is classed as non-variable (NV). The relatively large beamsize of the GB6 survey ($\approx 3.6 \times 3.4$ arcmin^2) means that confusion may be a problem; consequently any source for which the GB6 flux appears significantly greater than the flux density measured in Paper 1 may not be a true variable – where this is the case the class is marked with an asterisk in Table 4. (There are six sources with single epoch data only at either 1.4 or 4.8 GHz: three of these were not observed at 1.4 GHz in Paper 1 and three were too faint to appear in the GB6 catalogue).

It can be seen that in spite of the failure to detect variability in the GPS objects at 15 GHz, a significant fraction (10 out of 24) of them show evidence for variability at 1.4 or 4.8 GHz. It may be that GPS objects are more variable at 1.4–4.8 GHz than at 15 GHz (although this would counter the expected trend that objects are generally more variable at higher radio frequency than at lower frequency, down to a gigahertz or so); it is, however, plausible that 3 yr is too short a time interval over which to detect GPS variability – we see them as variable at 1.4 or 4.8 GHz simply because of the longer time-scales provided by the NVSS and GB6 surveys.

As discussed in Section 6.1, in the variability study presented here, five of the six HFP sources from the 9C complete sample are found to be variable at 15 GHz and the sixth shows longer term variability in the NED archive data. In addition, seven other HFP sources show variability at 1.4 or 4.8 GHz. Thus at least 13 of the 18 HFP sources are variable.

A source which has a peaked spectrum is likely to be strongly beamed rather than intrinsically young if it has any of the following properties: radio flux density variability over time-scales of a few years, association with a quasar, a flat or steep (rather than a rising) spectrum at frequencies below 1 GHz and structure on arcsecond scales. For each GPS and HFP source in samples A and B, NED has been used to provide lower frequency data and some optical information, and additional radio structural information has been obtained where possible from FIRST (Faint Images of the Radio Sky at Twenty centimeters; Becker, White & Helfand 1995). These data are summarized in Table 4. If a source has any of the properties listed above which are consistent with strong beaming rather than the youth scenario, it is labelled Y in Column 9 of Table 4 – Y? indicates that the source has possible evidence for beaming. Taking all these indicators into account the data show that 16 (possibly 21) of the 24 GPS sources and 15 (possibly 17) of the 18 HFP sources have properties which are consistent with strong beaming. Thus the evidence presented here indicates that the majority of the GPS and HFP objects present in samples selected at 15 GHz are objects dominated by emission from a strongly beamed self-absorbed component and are not necessarily intrinsically young objects.

7 CONCLUSIONS

A study of the 15-GHz variability of 51 9C sources over a 3-yr period has found no evidence for any variability (above $\sim$6 per cent flux calibration uncertainties) in steep-spectrum objects. Half of the 18 flat-spectrum objects were found to be variable. The HFP objects have been found to be highly variable – the majority (eight out of nine) exhibit variability at 15 GHz over a 3-yr period; archive data show that the ninth source is variable over slightly longer time-scales. None of the GPS objects were seen to vary at 15 GHz over 3 yr, but several show evidence of changing flux density over longer ($\sim$8–15 yr) time-scales in NED.

The majority of the GPS and HFP sources in the 9C survey are not resolved with resolutions of 3 mas with the VLBA. In particular,

Table 4. Properties of the GPS and HFP sources in samples A and B. Column 1: source name. Column 2: sample. Column 3: fitted peak frequency (see Paper 2). Columns 4–6: variability classes at 1.4, 4.8 and 15 GHz as defined in the text – * indicates that there may be a problem with confusion. Column 7: optical type: G – galaxy; G? – point-like object with $O - R \geqslant 1.6$ (see Paper 1); Q – confirmed quasar; Q? – point-like object with $O - R < 1.6$ (see Paper 1). Column 8: redshift. Column 9: evidence for beaming (properties as defined in the text): Y – yes; Y? – possibly. Column 10: notes.

Source name	Sample	Peak (GHz)	Variability (1.4 GHz)	Variability (4.8 GHz)	Variability (15 GHz)	Opt. type	Redshift	Beamed	Notes
GPS sources									
J0019+2956	A	1.2	PV	NV	NV	G	0.0244	Y?	
J0019+3320	A	1.2	NV	NV	NV	Q?	–	Y?	
J0020+3152	A	4.9	NV	NV	NV	U	–		
J0027+2830	A	1.1	V	NV	NV	G?	–	Y	
J0028+2954	A	4.4	V	NV	NV	G?	–	Y	
J0029+3244	A	1.0	PV	NV	–	G?	–	Y?	
J0032+2758	A	4.0	V	–	–	G	–	Y	
J0925+3159	B	0.5	NV	NV	–	G?	–	Y	Steep spectrum below 1.4 GHz – 5 arcsec in extent
J0925+3127	B	3.3	V	V*	–	G?	–	Y	Flat spectrum below 1 GHz?
J0932+2837	A	2.1	NV	NV	NV	G	0.3033		
J0933+2845	A	1.6	NV	NV	NV	Q	3.4214	Y	
J0936+2624	B	4.2	NV	PV	–	Q?	–	Y	Steep spectrum below 1 GHz; core-jet 45 arcsec in extent
J0945+3534	B	4.0	NV	PV	–	Q	1.2721	Y	Flat spectrum below 1 GHz; 16 arcsec in extent
J0949+2920	B	2.1	V	NV	–	G	–	Y	
J0952+3512	B	3.9	V	NV	–	Q	1.8764	Y	28-arcsec core-dominated double
J0953+3225	B	3.3	V	V*	–	Q	1.57	Y	Flat spectrum below 1 GHz; core-jet(?) 30 arcsec in extent
J0958+2948	B	2.2	NV	NV	–	Q	2.75	Y	Core-jet(?) 14 arcsec in extent
J1530+3758	A/B	3.4	NV	NV	NV	G	0.1519		
J1531+4356	A	2.7	V	V	–	G	0.4520	Y	
J1547+4208	A/B	2.7	NV	PV	–	G	2.7442	Y?	
J1550+4536	A	3.5	NV	PV*	–	G	–	Y?	
J1553+4039	A	2.0	V	NV	–	Q	2.7526	Y	Steep spectrum below 1.4 GHz
J1554+4348	A	3.7	V	NV	–	Q	1.4393	Y	
J1556+4259	A/B	4.4	NV	NV	–	Q	1.7462	Y	
HFP sources									
J0003+2740	A/B	5.5	PV	NV	–	Q?	–	Y?	
J0003+3010	A/B	10.7	V	PV	–	G?	–	Y	
J0012+3353	A/B	36.9	V	NV	V	G?	–	Y	
J0024+2911	A/B	13.1	NV	–	V	Q?	–	Y	
J0919+3324	B	10.0	V	V	–	G?	–	Y	
J0931+2750	B	8.5	V	V	–	G?	–	Y	
J0935+2917	A	5.3	V	NV	V	Q?	–	Y	
J0936+3207	A	16.8	NV	PV	V	Q	1.151	Y	
J0955+3335	B	5.9	V	V	–	Q	2.500	Y	
J1506+4359	A/B	11.1	–	NV	–	Q	0.9198	Y	
J1506+4239	A/B	14.3	–	V	–	Q	0.587	Y	Flat spectrum below 1 GHz; core-jet (?) 20 arcsec in extent
J1510+4138	A	5.8	–	NV	–	U	–		
J1521+4336	A/B	6.1	V	V	–	Q	2.180	Y	
J1526+3712	A/B	6.8	NV	V	NV	G?	–	Y	Steep spectrum below 1 GHz; 3.5 arcsec in extent
J1526+4201	A/B	7.9	PV	–	–	G	–	Y?	
J1528+3816	A/B	60.7	NV	V*	V	G?	–	Y	
J1540+4138	A	7.8	PV	NV	–	Q	2.5171	Y	
J1554+4350	A	10.7	V	NV	–	Q	1.4393	Y	

none of the 11 HFP objects observed with the VLBA has been resolved. The GPS objects seen in the 9C survey have been found to be either very compact objects (less than 3 mas in projected angular extent) or core-dominated objects with extended envelopes with flat or steep spectra at low frequency (not true GPS candidates).

If the flat-spectrum objects are excluded, the GPS and HFP objects make up around 40–50 per cent of the sources in our 15-GHz flux-limited samples. If they are all compact young radio sources, they are much more common than simple lifetime arguments would suggest they should be.

Thus, individually and as a whole, the high-resolution observations, variability properties and lifetime arguments suggest that the GPS and HFP objects present in samples selected at 15 GHz are objects dominated by emission from a strongly beamed self-absorbed component and are not necessarily intrinsically young objects. This does not oppose the youth scenario but suggests that, although it is possible that genuinely young HFP and GPS objects might be found in high-frequency radio surveys, such surveys are not a particularly good starting point for searching for young objects because the contamination from beamed objects is so high.

ACKNOWLEDGMENTS

We thank the referee, Merja Tornikoski, for helpful comments.

This work has made use of the NED, which is operated by the JPL, California Institute of Technology, under contract with the National Aeronautics and Space Administration.

The NRAO is a facility of the National Science Foundation operated under cooperative agreement by Associated Universities, Inc.

REFERENCES

Becker R. H., White R. L., Helfand D. J., 1995, AJ, 450, 559
Bolton R. C. et al., 2004, MNRAS, 354, 485 (Paper 1)
Bolton R. C., Chandler C. J., Cotter G., Pearson T. J., Pooley G. G., Readhead A. C. S., Riley J. M., Waldram E. M., 2006, MNRAS, 367, 323 (Paper 2)
Condon J. J., Cotton W. D., Greisen E. W., Yin Q. F., Perley R. A., Taylor G. B., Broderick J. J., 1998, AJ, 115, 1693
Gregory P. C., Scott W. K., Douglas K., Condon J. J., 1996, ApJS, 103, 427
Hughes P. A., Aller H. D., Aller M. F., 1992, ApJ, 396, 469
Jones M. E., 1991, in Cornwell T. J., Perley R., eds, ASP Conf. Ser. Vol. 19, Radio Interferometry – Theory, Techniques and Applications. Astron. Soc. Pac., San Fransisco, p. 395
O'Dea C. P., 1998, PASP, 110, 493
Owsianik I., Conway J. E., Polatidis A. G., 1999, New Astron. Rev., 43, 669
Peng B., Kraus A., Krichbaum T. P., Witzel A., 2000, A&AS, 145, 1
Pooley G. G., Fender R. P., 1997, MNRAS, 292, 925
Simonetti J. H., Cordes J. M., Heeschen D. S., 1985, ApJ, 296, 46
Snellen I. A. G., Schilizzi R. T., Miley G. K., de Bruyn A. G., Bremer M. N., Röttgering H. J. A., 2000, MNRAS, 319, 445
Taylor A. C. et al., 2003, MNRAS, 341, 1066
Tinti S., Dallacasa D., Stanghellini C., Celotti A., Publ. Astron. Soc. Aust., 2003, 20, 110
Tinti S., Dallacasa D., De Zotti G., Celotti A., Stanghellini C., 2005, A&A, 432, 31
Torniainen I., Tornikoski M., Teräsranta H., Aller M. F., Aller H. D., 2005, A&A, 435, 839
Tornikoski M., Jussila I., Johansson P., Lainela M., Valtaoja E., 2001, AJ, 121, 1306
Waldram E. M., Pooley G. G., Grainge K. J. B., Jones M. E., Saunders R. D. E., Scott P. F., Taylor A. C., 2003, MNRAS, 342, 915

This paper has been typeset from a TEX/LATEX file prepared by the author.